Measurement and Calculation of the Stark-Broadening Parameters for the Resonance Lines of Singly Ionized Calcium and Magnesium†

W. W. Jones,* A. Sanchez, J. R. Greig,‡ and Hans R. Griem
Department of Physics and Astronomy, University of Maryland, College Park, Maryland 20742
(Received 12 January 1972)

The electron-impact-broadened profiles of the resonance lines of singly ionized calcium ($\lambda \sim 3934$ Å) and magnesium ($\lambda \sim 2802$ Å) have been measured using an electromagnetically driven shock tube and a rapid-scanning Fabry-Perot spectrometer. For $N_e \simeq 10^{17}$ cm^{-3} and $T \simeq 19\,000$ °K, we found the Lorentzian half-width of the Ca^+ line to be 0.086 Å ± 10% and of the Mg^+ line to be 0.044 Å ± 10%. Using the quantum-mechanical theory of Barnes and Peach and our semiclassical calculation for the calcium lines, we found that the temperature dependence of the theoretical curves is close to that measured, although both theories predict actual values which are somewhat large. Using the quantum-mechanical theory of Bely and Griem and our semiclassical calculation for the magnesium lines, once again we found that the shape of both curves agrees quite well with the experimental points, although the quantum-mechanical predictions are somewhat too small. The probable sources of error are the use of the classical assumption in the semiclassical calculations and the use of an incomplete set of perturbing levels in the quantum-mechanical calculations.

I. INTRODUCTION

At present, the theory and measurement of Stark-broadening parameters of atomic systems, which can be used to deduce the environment of the radiating species, is quite successful for hydrogen atoms, hydrogenic ions (principally ionized helium), and neutral atoms, at least for those atomic systems which have a sufficiently complete energy-level structure available for calculations. However, in order to use the Stark effect in a more general way, say for the diagnosis of a high-temperature plasma, it will be necessary to extend our understanding of this effect to multiply ionized, but not necessarily hydrogenic, atoms. We have therefore measured the Stark widths (in this case due primarily to electron-impact broadening) of two of the simplest ion lines available, namely, the resonance of singly ionized magnesium and calcium. We have chosen these two lines since, owing to some recent theoretical developments,[1] it now seems possible to do fairly accurate semiclassical calculations,[2] as well as fully quantum-mechanical close-coupling calculations.[3,4]

II. THEORY

In the parameter range of interest, namely, $T \approx 19\,000$ °K and $N_e \approx 10^{17}$ cm^{-3}, electron-impact broadening dominates over van der Waals and (quasistatic) ion broadening, an assertion which will be justified later. Making this assumption, we have for width and shift of an "isolated" line

$$w + id = \langle if | \, | \sum_j f_j (1 - S_{ij} S^{\dagger}_{fj}) | \, | if \rangle \qquad (1)$$

in terms of the scattering matrices S for the scattering of electrons by ions. The expression $\langle i \| S \| i \rangle$ represents a reduced (in the sense of the Wigner-Eckart theorem[5]) matrix element of the scattering matrix S in the doubled line space $|if\rangle$. This expression is averaged over types of perturber collisions where $\sum_j f_j$ is given by

$$\sum_j f_j \rightarrow 2\pi N_e \int_0^{\infty} v f(v)\, dv \int_{\rho_{\min}}^{\infty} \rho\, d\rho (\cdots) \qquad (2a)$$

$$\rightarrow \pi N_e \left(\frac{\hbar}{m}\right)^2 \int_0^{\infty} dv \frac{f(v)}{v} \sum_{j,j'} (\cdots), \qquad (2b)$$

and Eq. (2a) is used for the semiclassical calculation and Eq. (2b) for the quantum-mechanical calculations. The velocity distribution $f(v)$ is usually taken to be Maxwellian.

We now consider two calculations of this expression [Eq. (1)]. The first is a semiclassical calculation based on a perturbation expansion of S. In doing this calculation, we have assumed that the odd-order terms in the perturbation expansion vanish.[6] There is still some question as to whether or not the first-order monopole term is canceled by ion effects (plasma polarization), but as we are interested primarily in the width, and since plasma polarization (a negative average space charge surrounding the ion) contributes primarily to the imaginary term in Eq. (1), it will not be discussed here. This semiclassical calculation is used to make a direct comparison between theory and experiment. The second calculation is a simplified quantum-mechanical argument, where the width part of Eq. (1) is rewritten in terms of total electron scattering cross sections.[7] This calculation is used primarily to show that the set of levels used in the calcium close-coupling calculation[3] is probably not sufficient. We have also done this calcula-

tion in a fully quantum-mechanical treatment in order to include the interference of the upper and lower levels, and the results confirm the findings of the second calculation; however, as we used the Coulomb-Born approximation to calculate the S matrix elements,[8] we did not attempt the calculation at low perturber energies ($k^2 \sim 0.2$ Ry) and the results are not presented here.

The emphasis in the quantum-mechanical calculation will be on the calcium results since the three-state approximation should lead to more serious errors for this case than for the magnesium results. This view is supported by our semiclassical calculations.

As we are dealing only with electron-impact broadening, we assume that the line profile is symmetric about the point $\omega_0 - d$. This approach can be modified if the ions prove to have a considerable effect on the line profiles.[6,9]

Our notation is that i refers to the initial state, f to the final state, and i', f' to the respective interacting states. We also use the usual definition of the shift and width, namely, the shift is the distance of the profile maximum from the position of the unperturbed line ($N_e \to 0$), and the width is half of the separation between the two half-intensity points.

A. Semiclassical Calculation

A semiclassical calculation is done by making a perturbation expansion for S and using, in general, only the first nonvanishing term in the perturbation (Dyson-series) expansion. This actually involves three terms: a second-order term affecting only the upper and lower states plus an interference term which is the product of two first-order terms. This procedure inherently treats only the weak interactions. In order to account for strong collisions (when the perturber and atomic electron wave functions overlap), which obviously cannot be done by a classical calculation, we must make some estimate for this effect and ensure that we still retain agreement in various limiting cases, e.g., in the adiabatic limit.[10] The calculation of this term, the use of straight rather than hyperbolic classical paths for the perturbers,[9] and the use of an incomplete set of perturbing (atomic) levels have been the prime sources of error (factors of ~2) in previous calculations.[9,11-13] A complete and self-consistent application of this theory is given in Ref. 2. The predictions from this theory for the widths and shifts of the calcium- and magnesium-ion resonance lines are summarized in Table IV below.

B. Simplified Quantum-Mechanical Calculation

To check the validity of using a limited set of perturbing levels in the close-coupling calculation we used a simplified expression for the width in terms of total cross sections σ_T.[14] This expression is

$$w \sim [\tfrac{1}{2} N_e v(\sigma_{T,i} + \sigma_{T,f} - \text{interference term})]_{\text{av}} . \quad (3)$$

We did the calculation for calcium, where the ($4S$-$4P$-$3D$) set of levels was used in the close-coupling calculation.[3] The results for calcium, using the Coulomb-Born approximation to calculate σ, are listed in Table I. As can be seen, the contribution from the $4D$ level is not negligible, and thus the use of the restricted set of levels ($4S$-$4P$-$3D$) is possibly not sufficient. Unfortunately, the predicted widths are already somewhat too large and as adding more perturbing levels should tend to increase w (we confirmed this by doing a complete quantum-mechanical calculation), the agreement will probably become worse. In principle the situation should be similar for magnesium, where the set of levels ($3S$-$3P$-$3D$) was used and the $4S$ level has been ignored; however, due to the change in principal quantum number, this effect will be much less. Also the theoretical predictions are somewhat low and thus adding more perturbing levels, which should tend to increase the width, should improve agreement between theory and measurement.

A problem which might affect calcium more than magnesium is the effect of resonances in the scattering cross sections. This effect will be discussed in more detail later.

III. LINE PROFILE MEASUREMENTS

A. Light Source

To obtain the densities and temperature where the Stark effect is the predominant line-broadening mechanism for the calcium and magnesium ions [$N \sim 10^{17}$ cm^{-3} and $T \sim 20\,000$ °K] we used an electromagnetically driven shock tube similar to that used by Lincke and Griem.[15] There was one major difference in the driving end of the T tube. To obtain a more homogeneous and reproducible plasma, we used a $1\frac{1}{2}$-in.-diam Pyrex T piece with a $\frac{3}{4}$-in. expansion tube in a "cookie-cutter" arrangement similar to that used by Berg.[16] By using a larger, slower capacitor with an external inductor in the

TABLE I. Cross sections from the unitarized Coulomb-Born approximation for Ca^+ at $k^2 = 0.7$ Ry (in units of πa_0^2).

	Inelastic			Elastic	
	SD	*PD*	*SP*	*SS*	*PP*
$4S$-$4P$-$3D$	2.76	39.25	37.96	28.17	103.34
$4S$-$4P$-$4D$	3.08	37.96	same	same	same
$4S$-$4P$-$5D$	0.53	···	same	same	same

discharge circuit [see Fig. 1(a)] we increased the useful life of the plasma, as well as obtaining a more homogeneous plasma. With the 14-μF capacitor charged to 18 kV and with a filling pressure (in the expansion tube) of between 0.5 and 1.5 Torr of the carrier gas consisting of ~90% helium and ~10% atomic hydrogen, the desired conditions were obtained. It was found that the density and temperature were not particularly sensitive to the filling pressure, but both were quite sensitive to the initial capacitor voltage. For the latter reason we used a sensing device to switch off the charging circuit [Fig. 1(a)] at a preselected voltage. Its sensitivity was better than 0.1%.

To fire the shock tube a 3-kV pulse was delivered to the trigger electrode of the high-voltage switch (in this case an ignitron, GE-7703). Since rise times less than 0.5 μsec were not required and since the maximum current was less than 35 kA, an ignitron sufficed quite well. An arc-heated plasma formed between the T-tube electrodes and, because of the current in the backstrap as well as pressure gradients, was projected along the expansion tube. A single sharp luminous front traveled down the expansion tube at ~1 cm/μsec. On reflection at a stainless-steel reflector ~14.5 cm from the electrodes the plasma was further heated and thermalized to form a macroscopically neutral, medium density, near LTE (local thermodynamic equilibrium) plasma. This assertion is justified later and of course is only required in a restricted sense. There is some question as to the precise mechanism of plasma heating under these conditions,[17] but we need not discuss this point here. It suffices to say that we obtained a slowly varying LTE plasma.[18]

The calcium and magnesium impurities are picked up by the plasma en route, because the tube was dusted with calcium or magnesium carbonate. There was always calcium in the plasma because of impurities in the expansion tube walls, but this was not sufficient. For the calcium runs we used a Pyrex expansion tube and for the magnesium runs a quartz (fused silica) expansion tube.

We checked for inhomogeneity in the distribution of helium (3889-Å total line intensity), of the electron density (continuum at 5360 Å), and of calcium (3934-Å total line intensity). We did this by measuring, side on, the light intensity for each wavelength at various chord lengths (distances from the tube axis) and "normalized" the signals by dividing the chord length into the signal. Since we used a very small solid angle, the signal was essentially from a narrow tube of plasma and the signal was integrated *along* the chord length. We also checked the shot-to-shot reproducibility (three shots had to be within 10% of each other at each chord length), and checked for clouding of the tube by returning to the starting position of the scan to compare the signals at the end of the run with those obtained initially (they were the same within reproducibility errors). Then by plotting these normalized intensities we obtained a measure of the inhomogeneity. There was a maximum change of 15% from the tube axis to the tube wall of any of the normalized intensities.

One precaution that was taken to reduce the level of (undesired) impurity radiation was to use a continuous flow gas system, the filling gas being metered by a needle valve. Another precaution was to ensure that the vacuum system would pump down to a base pressure well below the filling pressure;

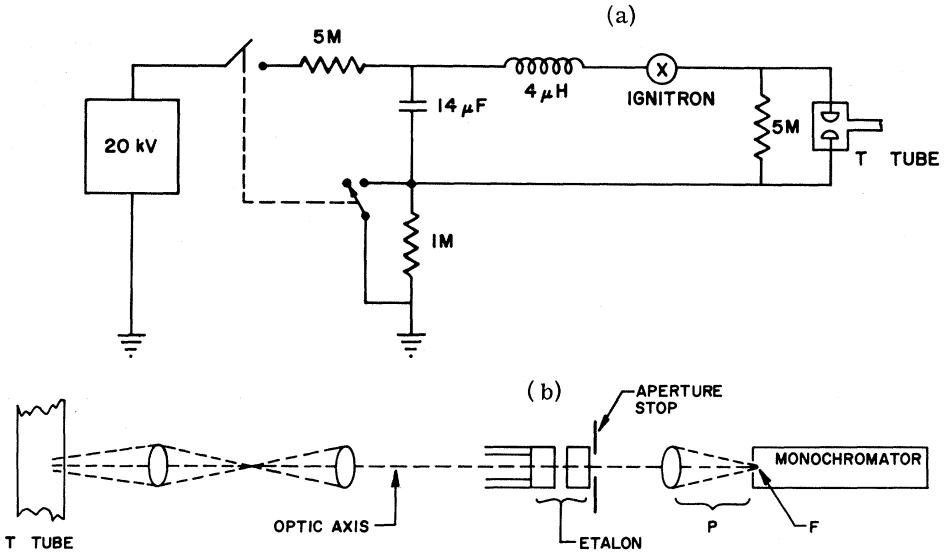

FIG. 1. (a) Charge-discharge circuit for the *T* tube. (b) Optical system used with the Fabry-Perot spectrometer.

i.e., with no filling gas, the pressure was at most 10^{-4} times the filling pressure. Finally, the reflector was made of stainless steel (as opposed to the usual aluminum). This was necessary because there is an aluminum resonance line [Al I (3944 Å)] very near the calcium ion line [Ca II (3934 Å)] we wished to study. Also we used a 10% admixture of hydrogen since this seemed to improve the reproducibility.

For complete LTE (i.e., down to the ground state) the collisional excitation rate must be much larger than the radiative excitation or deexcitation rate even for the first excited state. This condition[9] requires, assuming that the resonance lines of the main constituent are self-absorbed, that

$$N \gtrsim 10^{17}\left(\frac{E_2 - E_1}{E_H^z}\right)^3\left(\frac{kT}{E_H^z}\right)^{1/2} z^7 ,$$

which for neutral helium (the most stringent requirement) becomes

$$N \gtrsim 1.4\times 10^{16}\ \text{cm}^{-3} .$$

This requirement is satisfied in all cases. For LTE we also require that the time necessary for equilibration be less than a typical time, say, for a 10% variation in the plasma conditions during that part of the plasma lifetime in which we were interested. The appropriate time for equilibration between states n and $n+1$ is given by Eq. (67) of Griem[9] as

$$t \gtrsim \frac{4.6\times 10^7 z^3}{n^4 N_e}\left(\frac{kT}{E_H^z}\right)^{1/2}\exp\left(\frac{E_{n+1}^z - E_n^z}{kT}\right) ,$$

where the symbols are defined as in the reference. For the ground state and first excited states of neutral helium this formula yields

$$t \gtrsim 2.5\ \mu\text{sec} .$$

Since the typical time for plasma variation is ~ 2 μsec, this condition is barely satisfied for these levels but is well satisfied for all other levels of helium and hydrogen. (Note that we need not require LTE for Ca^+ or Mg^+ and that the helium ground-state populations do not enter into the analysis of the plasma conditions.)

B. Measurement Apparatus

To measure the narrow Ca^+ and Mg^+ resonance lines (0.03–0.3 Å), we use a rapid scanning Fabry-Perot spectrometer.[19,20] Details of this spectrometer, including machine-shop drawings and circuit diagrams for the associated electronics, as well as details of its use are available.[21] Briefly, the Fabry-Perot spectrometer consists of a simple etalon with one of the plates cemented to a metallic plate and the other cemented to a piezoelectric transducer. We use a tube of PZT-4 (Clevite Corp.) for the transducer 6 in. long, 1 in. outside diameter and $\frac{3}{4}$ in. inside diameter. The inner and outer cylindrical surfaces were coated with silver and the ceramic was polarized radially. Thus when a voltage is applied between the silvered surfaces, there is a lengthwise expansion. When the transducer is driven at its lengthwise resonant frequency (~ 10.5 kHz), relatively large amplitude oscillations are achieved. As the moving plate passes through its equilibrium (zero displacement) position, its velocity is easily sufficient to move a distance $\frac{1}{2}\lambda$ corresponding to one free spectral range in $\lesssim 1$ μsec, which was sufficient for our purposes. As described earlier, the duration of the plasma had purposely been lengthened so that over a period of ~ 2.0 μsec conditions remained approximately constant. Typically the Fabry-Perot system was adjusted so that a complete line profile was recorded in this time, and thus we could record several useful profiles per discharge.

For the calcium measurements an etalon made of borosilicate glass was used. These plates were coated with a dielectric coating and were nominally flat to $\frac{1}{50}\lambda$ at $\lambda = 5000$ Å. For the magnesium measurements, the etalon had to be made of fused silica plates. They too were coated with a dielectric coating but were nominally flat to $\frac{1}{200}\lambda$ at $\lambda = 5000$ Å. In both cases, the plates were 1 in. in diameter and 6 mm thick. Table II gives the parameters for the coatings at the wavelengths of interest. In both cases, the back surface of each plate is coated with a $\frac{1}{2}$% antireflection coating.

A complete analysis of the Fabry-Perot spectrometer in terms of its optical properties was given by Chabbal.[22] The additional effects caused by rapid scanning in this particular way were described by Copper and Greig[19,20] and in more detail by Greig.[23] The response of the Fabry-Perot system to monochromatic light is known as the instrument profile, and the finesse of the spectrometer (N_s) is given by

TABLE II. Measured coating parameters and finesses for the Fabry-Perot etalons used.

Element	λ (Å)	Material	Thermal coef./°C	Reflectivity (%)	Transmission (%)	Absorption (%)	N_s
calcium	3934	borosilicate	5.0×10^{-6}	~78	~18	~4	12.9
magnesium	2802	fused silica	0.4×10^{-6}	~75	~21	~4	10.9

$$N_s = \Delta\lambda_1 / \Delta\lambda_I = N_E \oplus N_F ,$$

where $\Delta\lambda_I$ is the half-width of the instrument profile and $\Delta\lambda_1$ the free spectral range. The latter is, in terms of plate spacing d and wavelength λ, given by

$$\Delta\lambda_1 = \lambda^2/2d ,$$

i.e., by the minimum wavelength difference between two monochromatic rays which may pass axially through the spectrometer with a fixed etalon spacing. The symbol $\oplus$ indicates the finesse (on the left-hand side) which would result from the convolution of the two functions whose finesses are given on the right-hand side of the equation.

Chabbal[22] separated the sources of instrumental broadening into components and defined a finesse due to each. The finesse of the etalon itself (N_E) divides into two components, one due to the reflectivity R of the etalon

$$N_R = \pi R^{1/2}/(1-R) ,$$

and the other due to the surface defects of the etalon (N_D). The subcomponents of N_D are the *static* curvatures (bowing) of the plates, the surface defects due to irregularities in the surface and its coating, and finally lack of parallelism. Functions for each of these convolve to form the etalon function,

$$N_E = N_R \oplus N_D .$$

The finesse due to reflectivity is fixed for the plates and wavelengths of interest (Table II). We found that we could eliminate the surface defects as a source of error simply by adjusting the plates until no change in the line separation or width (particularly of the central maximum) was detectable by eye over the useful portion of the etalon. We ensured this by doing the adjustment for the entire plate (~1.5 cm) and then using an aperture stop of ~3 mm. This procedure, as described in detail by Bradley,[24] yielded a surface defects finesse of $N_D \gtrsim 60$. Thus we have

$$N_E \rightarrow N_R .$$

Next we have the effect of the scanning system, which in our case [Fig. 1(b)] was determined by a lens of focal length F and the scanning aperture of diameter P. This finesse is defined by

$$N_F = 8(\Delta\lambda_1/\lambda)(F/P)^2 .$$

The choice of parameters was influenced by constraints imposed by the monochromator; namely, that for a given monochromator with a given dispersion we needed entrance and exit apertures to (i) eliminate nearby lines, (ii) have the monochromator function flat over the entire width of the line so that changing $\Delta\lambda_1$ would not affect the instrument profile (to simplify the deconvolution process), and (iii) have both apertures large enough to allow enough photons through so that we would not have noise problems. This led us to the choice of $F = 100$ mm, $P = 0.5$ mm for the calcium measurements and $F = 140$ mm, $P = 0.1$ mm for the magnesium measurements. In both cases we had

$$N_F > 60 .$$

We do not associate a finesse with the recording system (although Chabbal did), but we did calculate its effect on a theoretical function. The predominant effect was due to the integration circuit ($\tau \sim 0.03$ μsec) in the termination of the coax lines from the photomultiplier to the oscilloscope. It changed a Voigt profile of 0.4-sec half-width by ~2%. This too is negligible, leaving us with the instrument width determined by the reflectivity and by possible dynamic effects:

$$N_s \simeq N_R .$$

The dynamic effects are bowing owing to moving a glass plate cemented at its edges and Doppler shifts of the wavelengths owing to the moving plates. This last effect is negligible and will not be considered here (the requirement is that $V \ll 3$ km/sec). We cannot, *a priori*, calculate the effect due to the dynamic bowing; however, we can minimize its effects by using an aperture stop, reducing the effective diameter of the etalons from 1.5 to 0.3 cm, and by scanning the profile when the piezoelectric crystal is near its equilibrium position. Under these conditions, we found the finesse of the system [Fig. 1(a)] to be $N_s \sim 10$–12 in the resonant mode and $N_s \sim 11$–13 in the slow-scanning mode. Thus we have only a small broadening of the instrument profile because of dynamic bowing.

Since it is possible to have the finesse of the system change in the resonant mode (as demonstrated above), we found the instrument profile under actual operating conditions by choosing the system parameters so that the calcium (or magnesium) lines appeared to be monochromatic. We can assume (because of the choice of the parameters previously discussed) that the instrument profile does not change as the plate separation d is changed. Then, since $\Delta\lambda_1 \propto 1/d$, we merely decrease d until

$$\Delta\lambda_1 \gg \text{linewidth} .$$

A profile taken under these conditions yields an instrument profile. Then we scan with successively larger values of d until the experimental profiles begin to overlap (called order overlap). This yields a set of profiles of increasing accuracy, whose width, when deconvolved, must be consistent (if they were not then some function would not have been considered). We checked this in *each* run and found it to be true.

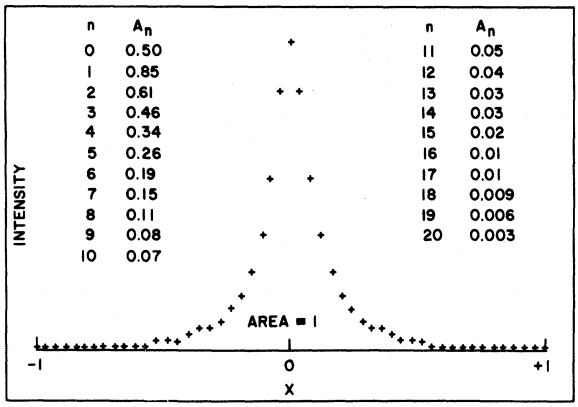

FIG. 2. The inverse transform of the instrument profile used in deconvolving the Stark profile from the total experimental profile. This represents the average of several profiles. (At least four were used for each run.) Plotted in the reduced wavelength scale $x = 2(\lambda - \lambda_0)/\Delta\lambda_1$.

A problem occurred in the initial runs with this choice of system parameters and with the monochromators available. We attempted a low-temperature (~10 000 °K) measurement to corraborate with Chapelle and Sahal-Brechot,[11] but the conventional shock tube we were using as a source had aluminum diaphragms. As mentioned previously, there is an aluminum resonance line [Al I(3944 Å)] so close to the calcium line [Ca II(3934 Å)] as to interfere with the (effective) instrument profile. For this reason we consider our preliminary results[25] to be suspect. This problem also occurred in the high-temperature measurements ($T \sim 20\,000$ °K in an electromagnetically driven shock tube), until we replaced the aluminum reflector with one made of stainless steel.

C. Data Reduction

The result of an experiment is a set of profiles for several values of d with each d value having profiles at several densities corresponding to different times in the life of the plasma. Then using the instrument profile (actually four or five profiles averaged together—see Fig. 2) we can reduce the experimental profile by numerical deconvolution. This yields a set of values for the Lorentz half-width w_l, which, when normalized to $N \sim 10^{17}$ cm^{-3}, should be self-consistent.

The method of reducing the data is similar to that of Larson and Andrew[26]; the primary differences are that we work in wavelength space while they worked in frequency space, and that we allow for asymmetries in the instrument profile by explicitly including the Fourier sine series. We start by normalizing the *instrument* profile to unit area, which is allowable since in all cases these profiles vanish on the wings, and then find its Fourier series using

$$I(x) = \frac{A_0}{2} + \sum_{n=1}^{n_{\max}} [A_n \cos(n\pi x) + B_n \sin(n\pi x)] ,$$

where

$$A_n = \int_{-1}^{+1} I(x) \cos(n\pi x)\, dx ,$$

$$B_n = \int_{-1}^{+1} I(x) \sin(n\pi x)\, dx ,$$

$$x = \text{reduced wavelength} = 2(\lambda - \lambda_0)/\Delta\lambda_1 ,$$

and $I(x)$ is the instrument profile in the reduced wavelength scale. We now have a check on the instrument profile since, if our understanding of the apparatus (see Sec. III B) is correct, the B's should approximately vanish. In our experiments they were *always* very close to zero. $n_{\max}$ was chosen by stopping the sum when $A_{n_{\max}} < 0.01 A_0$. This usually involved about twenty coefficients (Fig. 2). We can now convolve this series with a Voigt profile (to allow for Doppler broadening as well as Stark broadening), and by comparing this theoretical profile with our experimental profile we should be able to deduce the best value of w_l.

After convolving the instrument function (the above Fourier series) with a Gaussian function

$$G(x) = (1/g\sqrt{\pi})\, e^{-(x/g)^2} ,$$

where

$$g = \frac{2w_g/\Delta\lambda_1}{(\ln 2)^{1/2}} , \quad w_g = \lambda_0 (2kT \ln 2/MC^2)^{1/2} ,$$

for the Doppler profile and a Lorentzian function

$$L(x) = \frac{1/l\pi}{1 + (x/l)^2} , \quad l = \frac{2w_l}{\Delta\lambda_1} ,$$

for the Stark profile, we obtained the following function,[26] normalized to unity at $\lambda = \lambda_0$, i.e., at the line center:

$$\phi_{\text{theor}}(x) = \frac{\frac{1}{2}A_0 + \sum [A_n \cos(n\pi x) + B_n \sin(n\pi x)]\, e^{-(n\pi g/2)^2} e^{-n\pi l}}{\frac{1}{2}A_0 + \sum A_n\, e^{-(n\pi g/2)^2} e^{-n\pi l}} .$$

We used unity midpoint normalization for our theoretical (total) profile since it is not strictly necessary for the *experimental* profiles to vanish at the edge of the bandpass of the Fabry-Perot, and in fact, the base line was nonvanishing by 5–10% in some cases where more than instrumental broadening was present. Unity midpoint normalization is the simplest way to allow for this fact. This is a particularly judicious choice since the center of the profile will have the least error from photon noise. We can now select the Lorentzian width w_l by assuming that the best value will minimize the sum of squares of the deviations between the theoretical and experimental profiles, summed over all measured points.

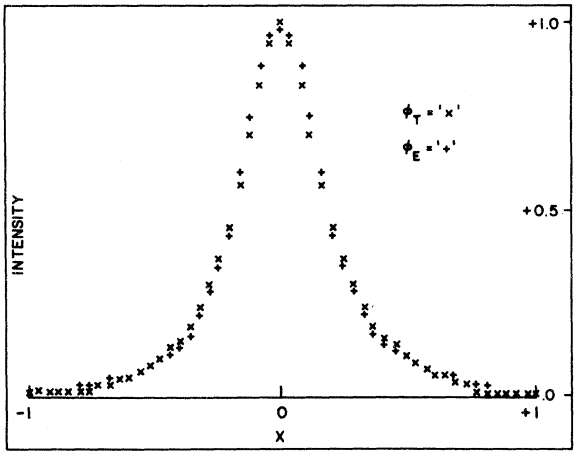

FIG. 3. Output from the computer program showing $\phi_{\text{theor}}(x)$: x, and $\phi_{\text{expt}}(x)$: +. Plotted in the reduced wavelength scale $x = 2(\lambda - \lambda_0)/\Delta\lambda_1$.

We started the data reduction by subtracting off a continuum $I_c(x)$, which could vary linearly as a function of time, from the experimental profile $I_{\text{expt}}(x)$ so that

$$\phi_{\text{expt}}(x_i) = I_{\text{expt}}(x_i) - I_c(x_i) .$$

The parameters we then varied were the Lorentzian half-width l of $\phi_{\text{theor}}(x)$ and the base line of $\phi_{\text{expt}}(x)$. This procedure allows for both a continuum background and for order overlap, provided the latter is not too serious. To check this assertion, we added together three profiles with Lorentzian half-widths of $l = (0.30, 0.10, 0.00)$ each separated by $\Delta\lambda_1$. We then asked the computer program to reduce the center profile. It obtained the value $l = 0.1007$, which is only ~0.1% in error. It is important to note that this procedure works only so long as the intensity at the limits of the Fabry-Perot bandpass, $\lambda_0 \pm \frac{1}{2}\Delta\lambda$, is no more than, say, 10% of the midpoint value. Thus we used as a criterion for selecting profiles a maximum of 10% for this value. Figure 3 shows a graph of the functions $\phi_{\text{theor}}(x)$ and $\phi_{\text{expt}}(x)$ and the reduced parameters.

D. Experimental Results

We obtain a self-consistent experiment by measuring the following data: the line profile of interest by using the Fabry-Perot spectrometer; the line profile of a He I line (3889 Å) for an electron density calibration; a He I (5016 Å) line-to-continuum ratio for a temperature measurement; and a continuum monitor synchronized with the Fabry-Perot output as another density calibration. The process of deconvolving the profiles requires a value for the temperature (both for the line of interest and for the He I density measurement) which is manifested in the Doppler profile, and although the temperature dependence is weak [i.e., a change of 5000 °K for the calcium measurements changes (w_l) by only ~2%], the correct temperature should yield the best fit of theoretical and experimental profiles. The line-to-continuum ratio, besides depending strongly on the temperature, has a considerable density dependence, as can be seen in Fig. 4. This complication is due to the presence of hydrogen in the gas mixture. Finally, the density calibration via the continuum has a weak dependence on the temperature where, in both cases, we are referring to the temperature and density regions of interest. Equations (2-59) and (14-12) of Ref. 9 were used in conjunction with a tungsten filament lamp to provide the density calibration. Equation (13-8) of the same source, modified to include hydrogen, was used for the line-to-continuum ratio to temperature conversion. The calcium and magnesium experiments are now described separately.

(*a*) *Calcium*: $\lambda = 3934$ Å, *transition* $= 4S_{1/2}$-$4P_{3/2}$, ^2S-^2P. There were three runs for which the results are listed in Table III, along with the final, averaged values, properly adjusted (see Secs. III E and III F). In the first run we had actually used the calcium resonance lines [Ca II (3934 Å)/Ca I (4226 Å)] for the temperature calibration, where Eq. (13-4) of Ref. 9 was used for the conversion. The

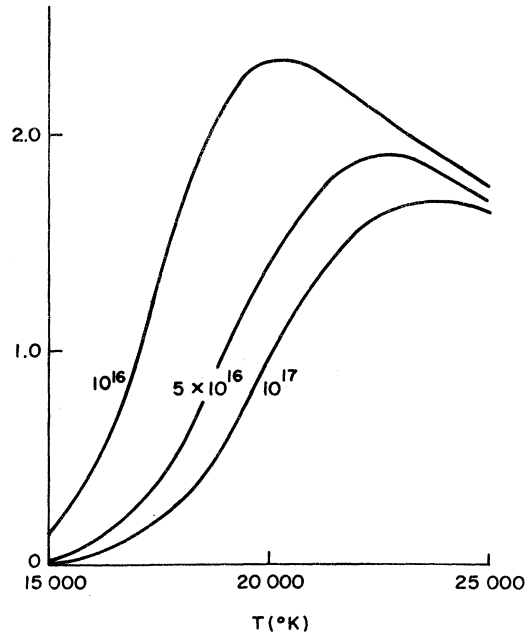

FIG. 4. Line-to-continuum to temperature calibration curve using a bandpass of 100 Å for the He I line at $\lambda \sim 5016$ Å.

TABLE III. Measured values for the Stark width of the calcium- and magnesium-ion resonance lines: w is the Lorentzian half-width, number of profiles averaged to obtain the measured value and a calculated error bar (see text); "final" is the weighted average corrected as estimated in Sec. III F.

Element	Run	Profiles used	w(Å)	Temperature
Ca^+	1	8	0.085(± 30%)	17 000(± 20%)
$\lambda \sim 3934$ Å	2	6	0.088(± 10%)	18 000(± 10%)
$4S_{1/2}$-$4P_{3/2}$, ^2S-^2P	3	4	0.084(± 12%)	20 000(± 15%)
	final	10	0.086(± 10%)	19 000(± 15%)
Mg^+	1	9	0.044(± 11%)	18 000(± 20%)
$\lambda \sim 2802$ Å	2	6	0.043(± 11%)	19 000(± 20%)
$3S_{1/2}$-$3P_{1/2}$, ^2S-^2P	final	15	0.044(± 10%)	18 500(± 20%)

continuum monitor had served for the density calibration. For the second run, more care was taken to choose profiles from a time period which had only small fluctuations in the density. The temperature was (to the accuracy needed) constant throughout the useful life of the plasma. In this case there was also a helium profile [He I (3889 Å)] measurement, using the Fabry-Perot spectrometer for the density calibration; however, as the monochromator instrument width was too narrow, the helium profiles yielded densities ~20–30% lower than the continuum monitor. The experiment was performed again, this time taking care to obtain useful helium profiles. The helium profiles and the continuum monitors then agreed to within ~4%. In both of these runs, the helium [He I (5016 Å)] line-to-continuum ratio was used for the temperature calibration. The run listed as "final" is the average of runs 2 and 3 including corrections for other broadening mechanisms.

(*b*) *Magnesium*: $\lambda = 2802$ Å, *transition* = $3S_{1/2}$-$3P_{1/2}$, ^2S-^2P. The magnesium runs were essentially the same as in runs 2 and 3 of the calcium experiment, except that, owing to experimental constraints, we were not able to use the helium profile as a check on the density calibration. This was due to using a monochromator with a very narrow, ~1.5-Å, bandpass to separate the magnesium resonance lines and a nearby multiplet ($3S$-$3P$ doublet at 2796, 2802 Å and $3P$-$3D$ doublet at 2790, 2798 Å). We did not consider this serious, since we had previously obtained such good agreement between the two methods. The results are listed in Table III. Once again "final" is the average of runs 1 and 2 with allowance made for other broadening mechanisms.

E. Error Analysis

There are two principal sources of error in our measurements of the line profiles. The most important error is systematic and comes from a slight inhomogeneity (~15%) in the electron density from the center of the expansion tube to the outside edge of the plasma. Since the ions (calcium and magnesium) are radiating throughout the plasma, we therefore assign the minimum error of ± 7% to the measurements. No matter how many profiles are measured, the error brackets can never decrease below this value. The other principal source of error is random in nature and comes from measuring profiles, where the absolute line intensity (and thus the number of radiating atoms), as well as the electron density, is varying in time. One criterion used for selecting profiles is that these variations be small. Then the distribution of measured points gives a mean value and an error bracket. These errors (due to random processes) are combined in the usual[27] way and then combined with the systematic error to yield the quoted error bars.

The other possible source of error is in the reduction process itself and could come from noise in either the experimental profile or the instrument profile, or from an uncertainty in the temperature. As previously mentioned, the temperature-associated error is small. Photon noise was also almost always small and even for those profiles in which it appeared that there might be a problem, the results were nevertheless consistent with the other values. External electromagnetic noise was nonexistent. These errors once again[27] can be combined to yield an error (measured by making changes in various parts of the deconvolution process) of ~2% per profile. This error will also be random, and as we used a large number of profiles for each case, we do not expect this to be a significant contribution to the total error bar.

F. Other Broadening Mechanisms and Corrections

To confirm the statement that in the region of interest, i.e., $N \approx 10^{16}$–10^{17} cm^{-3} and $T \approx 20\,000$ °K, Stark broadening and in particular electron-impact broadening dominates, we must estimate the error due to other broadening mechanisms, namely, resonance broadening, van der Waals broadening, and (quasistatic) ion broadening.

(*a*) *Resonance broadening*. Equation (4-104) of Ref. 9 yields $w < 10^{-18} N_{\text{ion}}$ (in cm^{-3}) Å. Since calcium and magnesium are impurity atoms only, and since the intensities of He I (3889 Å) and Ca II (3934 Å) and Mg II (2802 Å) were comparable, we can argue, using statistical mechanics and quantum-mechanical arguments, that $N_{\text{ion}} \ll N_e$ and thus estimate $w_{\text{res}}/w_{\text{expt}} < 0.001$, so that in neither case is this significant.

(*b*) *van der Waals broadening*. Using the most recent experimental values and temperature scaling laws for van der Waals broadening of calcium[28] we have $w \approx (T_2/T_1)^{0.28}\, 1.67 \times 10^{-30} \lambda^2 N_{\text{He I}}$ Å where $T_1 \approx 5000$ °K, which yields $w_{\text{vdW}}/w_{\text{expt}} \simeq 0.04$. A theoretical estimate [Ref. 9, Eq. (4-113)] shows that

TABLE IV. Compairson of measured and calculated Lorentzian half-widths for calcium- and magnesium-ion resonance lines. w_{expt} is the experimental half-width, w_{theor} is our semiclassical calculation (Ref. 2), w_{QM} is from the close-coupling calculations (Ref. 3 and 4), and w_{expt}/w_{QM} is the ratio of the experimental to quantum-mechanical half-widths.

Reference	Element	T (°K)	w_{expt} (Å)	w_{theor} (Å)	w_{QM} (Å)	w_{expt}/w_{QM}
Yamamoto (Ref. 27)		11500	0.050(± 12%)	0.147	0.115	0.43
Chapelle (Ref. 22)	Ca^+	12200	0.102(± 20%)	0.145	0.110	0.93
Our work	$\lambda = 3934$ Å	19000	0.086(± 10%)	0.125	0.095	0.91
Roberts (Ref. 28)		30000	0.051(± 17%)	0.119	0.082	0.63
Hildum (Ref. 31)[a]		18400	0.094(± 15%)	0.125	0.095	0.99
Chapelle	Mg^+	12500	0.056(± 20%)	0.048	0.035	1.60
Our work	$\lambda = 2802$ Å	18500	0.044(± 10%)	0.044	0.031	1.42

[a]The measurement of this line may have been affected by interference with the He I $\lambda = 3964$-Å line, as the 3968-Å rather than the 3934-Å line of the doublet was measured in the experiment.

the van der Waals width for magnesium is about 0.1 times that of calcium. As the experimental width of magnesium is about 0.5 times that of calcium for a given density, we have for the magnesium experiments $w_{vdW}/w_{expt} \simeq 0.01$.

(*c*) (*Quasistatic*) *ion broadening*. Using[9]

$$w_T = w[1.0 + 1.75\alpha(1.0 - 1.2r)],$$

with $\alpha < 0.01$, $r < 0.5$, or using an alternative estimate[6] for ion-quadrupole interactions, namely,

$$w_{iq} \simeq (\lambda^2/c)Na_0(\hbar/m)(n_i^2 - n_f^2),$$

we obtain, using either estimate, for both calcium and magnesium $(w_{qsi}/w_{expt}) \lesssim 0.015$, with w_{expt} representing the experimental width in all cases. Therefore we estimate a maximum downward correction of ~5% for calcium and ~3% for magnesium from these other broadening mechanisms.

(*d*) *Superposition*. Opposing these corrections is the effect of the superposition of Lorentz functions with different widths, where the width is a function of radius. Using an averaged profile

$$\bar{L} = \frac{1}{R}\int_0^R dr \frac{w(r)/\pi}{w^2 + \omega^2} \quad ,$$

and assuming that the density varies linearly from the tube axis to the tube wall, we find that for Δw (the change in the half-width across the tube) small compared to w

$$w_{true} \simeq w_{meas}(1 + \Delta w/2w) .$$

This expression then gives us the values at the mean density. As w is proportional to N_e, this upward correction about cancels the previously mentioned downward correction for calcium and leaves a residual correction of ~4% (upward) for magnesium, which is included in Table III.

IV. COMPARISON OF THEORETICAL AND EXPERIMENTAL RESULTS

A. Calcium ($\lambda \approx 3934$ Å)

Several calcium-ion resonance line measure-

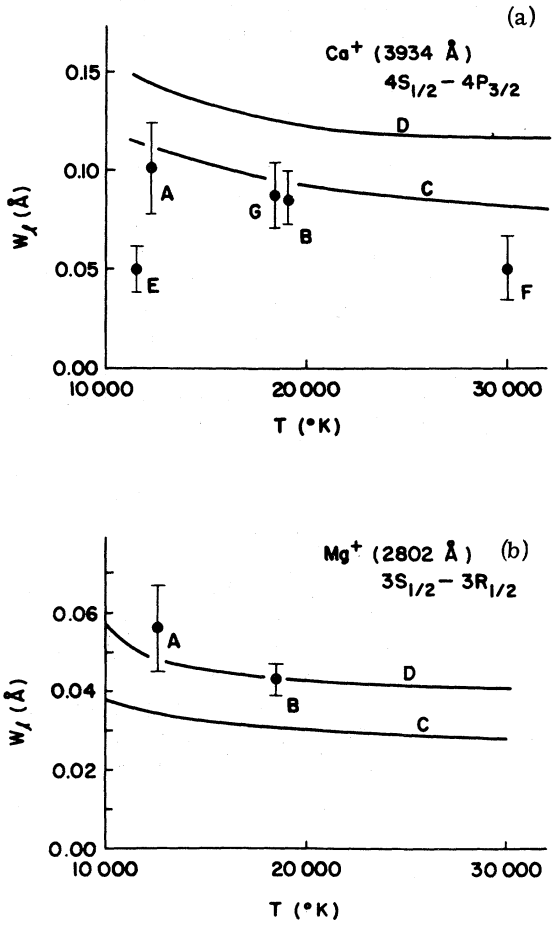

FIG. 5. Graphs showing the calcium (a) and magnesium (b) results; measured values are plotted with the experimental error bars as quoted by the respective authors. *A*, Chapelle and Sahal-Brechot (Ref. 11); *B*, our measurement; *E*, Yamamoto (Ref. 29); *F*, Roberts and Eckerle (Ref. 30). Also plotted are the close-coupling calculation of Barnes and Peach (Ref. 3) or Bely and Griem (Ref. 7) (*C*), and our semiclassical calculation (Ref. 2) (*D*). A recently measured point of Hildum and Cooper is also shown (*G*).

ments have been made so far[11,29-31] with widely varying conditions and with a variety of sources. However, all these measurements were made using conventional monochromators [except for Yamamoto[29] who used a Fabry-Perot etalon (method not explained) and Hildum and Cooper[31] who used a scanning Fabry-Perot]. These values, after normalization to $N_e = 10^{17}$ cm^{-3}, are shown in Table IV along with our semiclassical predictions.[2] The measured values seem to be consistent with each other except for the results of Yamamoto. Table IV also shows the ratio of the measurements to the quantum-mechanical calculation of Barnes and Peach.[3] The variation of this ratio gives an estimate of the "goodness" of the quantum results. Figure 5(a) shows the measured values (with quoted error brackets), the quantum results, and our semiclassical results.

B. Magnesium

The number of measurements of the linewidth of the resonance line of ionized magnesium is much smaller. Chapelle and Sahal-Brechot[11] measured the width (and shift) in an arc plasma at a low temperature ($T \sim 12\,500$ °K). We have made the corresponding width measurement in a T tube at a high temperature ($T \sim 18\,500$ °K). Both groups have done semiclassical calculations for this line, and Bely and Griem[4] have done the corresponding close-coupling calculation using the $\vec{R}$ matrices of Burke and Moores.[32] The results are summarized, as for calcium, in Table IV and Fig. 5(b).

V. CONCLUSIONS

Semiclassical calculations[2] seem to be fairly good for the magnesium-ion resonance lines, in spite of the small value of contributing angular momenta L of the colliding electron, but not so good for the calcium-ion resonance lines where these predictions are too large. The quantum-mechanical calculations for magnesium[4] fall somewhat short (a recent quantum-mechanical calculation[33] deviates by ~15% more in this direction), but the agreement between calculated and measured widths should improve with the inclusion of the 4s state and further improvement might, of course, be gained by using exactly calculated $\vec{R}$ matrices rather than extrapolated values. The quantum-mechanical calculations for the calcium lines[3] seem to be in good agreement with some measured widths, although at high temperatures the predicted widths seem somewhat too large. Unfortunately, the present agreement may be fortuitous. As pointed out above, an important (atomic) perturbing level has been ignored, namely the 4D level. The results of the simplified quantum-mechanical calculation (Sec. II B) shown in Table I indicate a possible 25% discrepancy, and our more complete calculations including an interference term indicate an even larger error. Thus, after inclusion of a complete set of perturbing levels, the widths calculated using a fully quantum-mechanical formulation may be no better for the calcium ion than our semiclassical calculation. A possible explanation for such difficulties for the calcium line lies in the large number of energy levels near the 4S and 4P energy levels. This leads to many more resonances in the scattering cross section, and since the relevant perturber energies (1–4 eV) are near these threshold energies, we should expect some uncertainty in the calculation. This is especially true if the calculation is carried out for energies above threshold and then extrapolated to energies below threshold.

An often used semiempirical (se) procedure[34] for the prediction of electron-impact broadening of isolated ion lines predicts widths in terms of an effective Gaunt factor g_{se}. Nominally at the temperature of interest ($T \sim 20\,000$ °K) we expect $g_{se} = 0.20$. Our measurements suggest a near-threshold value of $g_{se} = 0.20$ and $g_{se} = 0.32$ for the calcium and magnesium lines, respectively.[2] Such variations are well within the estimated theoretical errors of this simple method.

---

†Research supported by the National Aeronautics and Space Administration.

*Some of the material in this paper is part of a Ph.D. thesis (University of Maryland, 1971) (unpublished).

‡Current address: Imperial Chemical Industries, Ltd., Wexham Road, Slough, Bucks, England.

[1]S. Klarsfeld, Phys. Letters 33A, 437 (1970); see also S. Sahal-Brechot, Astron. Astrophys. 1, 91 (1969).

[2]W. W. Jones, S. Benett, and H. R. Griem, University of Maryland Technical Report No. 71-128, 1971 (unpublished).

[3]K. S. Barnes and G. Peach, J. Phys. B 3, 350 (1970).

[4]O. Bely and H. R. Griem, Phys. Rev. A 1, 97 (1970).

[5]B. Shore and D. Menzel, *Principles of Atomic Spectra* (Wiley, New York, 1968).

[6]H. R. Griem, *Broadening of Spectral Lines by Charged Particles*, (Academic, New York, to be published).

[7]M. Baranger, in *Atomic and Molecular Processes*, edited by D. R. Bates (Academic, New York, 1962).

[8]D. Petrini (private communication).

[9]H. R. Griem, *Plasma Spectroscopy* (McGraw-Hill, New York, 1964).

[10]D. E. Roberts and J. Davis, Phys. Letters 25A, 175 (1967).

[11]J. Chapelle and S. Sahal-Brechot, Astron. Astrophys. 6, 415 (1970).

[12]J. Cooper and G. K. Oertel, Phys. Rev. Letters 13, 530 (1967).

[13]H. R. Griem, Phys. Rev. Letters 17, 518 (1966).

[14]M. Baranger, Phys. Rev. 112, 855 (1958).

[15]R. Lincke and H. R. Griem, Phys. Rev. 143, 66 (1966).

[16]H. F. Berg (private communication).
[17]J. R. Greig and G. Palumbo, Phys. Fluids 12, 1211 (1969).
[18]T. N. Lie, M. J. Rhee, and E. A. McLean, Phys. Fluids 13, 2492 (1970).
[19]J. Cooper and J. R. Greig, J. Sci. Instr. 40, 433 (1963).
[20]J. R. Greig and J. Cooper, Appl. Opt. 7, 2166 (1968).
[21]W. W. Jones and J. R. Greig, University of Maryland Technical Report No. 943, 1969 (unpublished).
[22]R. Chabbal, J. Rech. Centre Natl. Rech. Sci. Lab. Bellevue (Paris) 24, 1386 (1953); we used an English translation by R. B. Jacobi, U.K.A.E.A., Harwell, England.
[23]J. R. Greig, dissertation (University of London, 1965) (unpublished).
[24]D. J. Bradley, J. Sci. Instr. 39, 41 (1962).
[25]W. W. Jones, H. R. Griem, J. R. Greig, and M. H. Miller, Bull. Am. Phys. Soc. 15, 1513 (1970).
[26]H. P. Larson and K. L. Andrew, Appl. Opt. 6, 170 (1967).
[27]H. Cramer, *Mathematical Methods of Statistics* (Princeton U. P., Princeton, N. J., 1966), p. 191.
[28]G. Hammond, dissertation (University of Maryland, 1971) (unpublished).
[29]M. Yamamoto, Phys. Rev. 146, 137 (1966).
[30]J. Roberts and K. R. Eckerle, Phys. Rev. 159, 104 (1967).
[31]J. S. Hildum and J. Cooper, Phys. Letters 36A, 153 (1971).
[32]P. Burke and D. Moores U.K.A.E.A. Report No. HL. 68/5695, Harwell, 1968 (unpublished).
[33]K. S. Barnes, J. Phys. B 4, 1377 (1971).
[34]H. R. Griem, Phys. Rev. 165, 258 (1968).

PHYSICAL REVIEW A VOLUME 5, NUMBER 6 JUNE 1972

Calculated Bremsstrahlung Spectra from Thick Tungsten Targets*

Ellery Storm
Los Alamos Scientific Laboratory, Los Alamos, New Mexico 87544
(Received 3 September 1971)

The bremsstrahlung energy distribution from a thick tungsten target is calculated from the Sommerfeld and Born-approximation thin-target formulas, taking into account electron energy losses, electron backscatter losses, and photon attenuation in the target. Over-all agreement with measurement is 20% in the 12–100-keV energy range, increasing to 50% at 300 keV. Semiempirical expressions are developed that give 20% over-all agreement with measurement in the 12–300-keV energy range.

I. INTRODUCTION

The x-ray spectrum produced by low-energy electrons striking a target is not only interesting theoretically but also because x rays are used extensively in medicine and industry. Ehrlich[1] compared thick-target bremsstrahlung theory to her measurements and found "order-of-magnitude agreement." Recently, absolute measurements by Unsworth and Greening[2] in the 15–30-keV energy range and by Storm, Israel, and Lier[3] in the 12–300-keV energy range have been reported. Previous measurements below 300 keV include those of Hettinger and Starfelt,[4] Dyson,[5] and Placious.[6] Sufficient experimental information is now available to permit a reevaluation of the thick-target bremsstrahlung theory.

The semiclassical formula of Kramers[7] has been used extensively to calculate thick-target spectra, although it neglects electron backscatter and photon attenuation losses. Unsworth and Greening[2] obtained agreement with their measurements by correcting the Kramers formula for photon attenuation.

Berger and Seltzer[8–10] have developed a Monte Carlo program for calculating bremsstrahlung spectra which includes electron and photon multiple scattering. Their calculations for normal incidence of the electron beam on the target are in good agreement with the measurements of Placious.[6] In the present calculation, thin-target bremsstrahlung formulas developed from quantum mechanics are corrected for electron energy losses, electron backscatter losses, and photon attenuation to obtain thick-target bremsstrahlung distributions that can be compared to measurement. Semiempirical equations also are compared to measurement, and one is developed that gives 20% agreement below 300 keV.

II. THIN-TARGET BREMSSTRAHLUNG FORMULAS

Bremsstrahlung cross-section theory has been developed either with Sommerfeld-Maue wave functions or in the plane-wave Born approximation. The thin-target bremsstrahlung formulas have been reviewed by Koch and Motz.[11] Of the formulas differential in photon energy, the Sommerfeld formula[12] and the formulas labeled 3BN and 3BN(a) by Koch and Motz are applicable below 300 keV. In